Naunyn-Schmiedeberg's Archives of Pharmacology (2024) 397:5631–5647
https://doi.org/10.1007/s00210-024-02965-4

RESEARCH

Exposure of piperlongumine attenuates stemness and epithelial to mesenchymal transition phenotype with more potent anti-metastatic activity in SOX9 deficient human lung cancer cells

Surya Kant Tripathi[1,2] · Rajeev Kumar Sahoo[1] · Bijesh Kumar Biswal[1]

Received: 8 December 2023 / Accepted: 15 January 2024 / Published online: 27 January 2024
© The Author(s), under exclusive licence to Springer-Verlag GmbH Germany, part of Springer Nature 2024

Abstract

Phytocompounds have shown hopeful results in cancer therapy. Piperlongumine (PIP), a naturally derived bioactive alkaloid found in our dietary spice, exhibits promising pharmacological relevance including anticancer activity. This study reconnoitred the anti-lung cancer effect of PIP and the allied mechanisms, in vitro and ex vivo. The cytotoxic, anti-proliferative, and apoptotic effects of PIP on lung cancer cells (LCC) were checked via cell viability, colony formation, cell migration, invasion, comet assay, and various staining techniques. Further, multicellular spheroids assay explored the anti-lung cancer potential of PIP, ex vivo. Preliminary results explored that PIP exerts selective cytotoxic and anti-proliferative effects on LCC by DNA damage and cell cycle arrest. PIP remarkably escalated the cellular and mitochondrial reactive oxygen species (ROS) generation and promoted dissipation of mitochondrial membrane potential (MMP), which triggers activation of caspase-dependent apoptotic pathway in LCC. Mechanistically, PIP showed F-actin deformation mediated significant anti-migratory and anti-invasive activity against LCC. Herein, we also found that F-actin dis-organization modulates the expression of epithelial to mesenchymal transition (EMT) markers and inhibits the expression of stemness marker proteins, like SOX9, CD-133, and CD-44. Moreover, PIP effectively reduced the size of spheroids with strong apoptotic and cytotoxic effects, ex vivo. This has been the first study to discover the high expression of SOX9 supporting the survival of LCC, whereas its inhibition induces higher sensitivity to PIP treatment. This study concludes a newer therapeutic agent (PIP) with promising anticancer activity against LCC by escalating ROS and attenuating MMP, stemness, and EMT.

Keywords Lung cancer · Piperlongumine · ROS · EMT · Stemness · SOX9

Introduction

Lung cancer represents the second most devastating and rapidly growing cancer worldwide (Sung et al. 2021). As per reports, lung cancer is at the top in terms of mortality, worldwide and is the 4th most leading cause for death in India (Sung et al. 2021). Most of the cases of lung cancer are detected at advanced stages, leading to poor diagnosis and increased incidence of cancer-related mortality worldwide (Sung et al. 2021). The cancer stem cells (CSCs) play an important role in cancer initiation, progression, metastasis, and drug resistance in lung cancer (Kim et al. 2020). The CSCs are resistant to conventional therapies and often lead to tumor recurrence, post therapy (Phi et al. 2018). During therapy, the CSCs can turn on multiple responses like epithelial to mesenchymal transition (EMT) induction and aberrant signalling pathways for their self-renewal. EMT is also known to spread lung cancer by losing contact inhibition, leading to the propagation of cancer cells and loss of apoptosis (Ye and Weinberg 2015). EMT also plays essential role in promoting stem-cell phenotype and therapy resistance in cancer (Ye and Weinberg 2015). Multiple dysregulated signalling pathways promote EMT and stem-cell phenotype, while conventional chemotherapeutics have limited outcomes and significant side effects on patients (Mittal 2016). Therefore, the search for effective agents with pleiotropic nature and those that can reverse EMT and stem-cell

✉ Bijesh Kumar Biswal
biswalb@nitrkl.ac.in

[1] Cancer Drug Resistance Laboratory, Department of Life Science, National Institute of Technology Rourkela, Rourkela 769008, Odisha, India

[2] Lineberger Comprehensive Cancer Centre, University of North Carolina, Chapel Hill 27514, NC, USA

phenotypes is currently needed. Studies have reported the effectiveness of nanocapsulated drug delivery molecules showing synergistic anticancer effects on lung cancer cells (Alagheband et al. 2022; Javan et al. 2022). A study reported the reversal of resistance through nanoparticle drug delivery in gastric cancer (Nejati et al. 2022). Along with these, many phyto-compounds are known for their pleiotropic nature and pharmacological application as therapeutics, including potent anticancer activity (Tripathi et al. 2019). In addition, phyto-compounds also show selective toxicity towards cancerous cells with minimal adverse effects (Tripathi et al. 2020). One such phyto-compound, Piperlongumine (PIP), a biologically active alkaloid-based ingredient of our dietary spices is a well-known phyto-compound commonly isolated from the plant *Piper longum* (Bezerra et al. 2013). PIP has been well reconnoitred for its medicinal properties, including anticancer activity (Ranjan et al. 2019). Previous studies on PIP suggested that the anticancer activity of PIP is primarily determined by the overproduction of reactive oxygen species (ROS) in cancer cells (Chen et al. 2019). Moreover, PIP has also shown anti-invasive and anti-migratory activities in various cancers. Song and colleague's study documented that PIP inhibits the proliferation, migration, and invasion of gastric cancer cells by obstructing JNK1,2/STAT3 phosphorylation (Song et al. 2016).

Furthermore, PIP has been known for stemness suppressive activity via inhibiting the regulatory proteins of stemness in oral cancer (Chen et al. 2018). Studies have reported that transcription proteins play major role in both cancer progression and prevention (Pouremamali et al. 2022). Sex-determining region Y (SRY)-related high mobility group (HMG) box-9 (SOX9), a prominent transcription factor of the SOX family, has a crucial role in the process of embryonic development (Panda et al. 2021). SOX9 can potentially activate many auto-regulatory functions associated with the maintenance of stem cell state (Belo et al. 2013). In contrast, deregulation in SOX9 activity is related to many consequences like initiation and progression of the cancer cell proliferation, invasion, migration, metastasis, and maintenance of stem-cell phenotype in cancer progenitor cells (Panda et al. 2021; Tripathi et al. 2022). In breast cancer, overexpression of SOX9 promotes stemness, poor prognosis, and tamoxifen resistance via targeting ALDH1A3 (Domenici et al. 2019), while silencing of SOX9 inhibits cancer cell proliferation and auto-renewal by preventing the activation of β-catenin signaling pathway leading to senescence and apoptosis (Domenici et al. 2019).

The current study explores the mechanisms involved in PIP-induced cytotoxicity and anti-tumorigenic activity on human lung cancer cells as well as multicellular spheroids. We have further investigated the effect of PIP on mitochondrial membrane potential (MMP), mitochondrial ROS, DNA damage, and EMT. Lastly, we have assessed the influence of the compound on invasion, migration, and stem-cell phenotype in SOX9 knockdown lung cancer cells.

Material and methods

Cell lines and cell culture

Lung cancer cell lines, A549 and NCI-H522, were bought from the National Centre for Cell Science, India. Another cell line, HaCaT, was received from Prof. S.K. Patra, NIT Rourkela. Cell lines were cultured in DMEM with 10% FBS at 37 °C in 5% CO_2 and used in all the experiments.

F-actin cytoskeleton staining

Cells were treated with PIP at desired concentrations for 48 h. Cells were fixed with 4% paraformaldehyde (PFA) and incubated with 0.1% Triton X-100. Cells were stained with Alexa Fluor™ 488 phalloidin (Thermo-Fisher Scientific, USA), followed by Hoechst 33,342. The variations in F-actin cytoskeleton filament were analyzed using a fluorescence microscope (Olympus, Japan) (Nayak et al. 2021).

Cell viability assay

Cells were cultured in 96-well plate and desired treatment was given for 24, 48, and 72 h. MTT solution (0.5 mg/ml) was added, followed by DMSO after 4 h incubation. The absorbance was taken at 570 nM in an ELISA microplate reader (Biotek, USA). The detailed protocol has been mentioned in our previous published article (Tripathi and Biswal 2018).

Wound healing migration assay

Cells were cultured to form a monolayer and incubated under serum-starvation conditions for 24 h to bring it to a uniform stage. A scratch was marked using a sterilized 200 µl tip and PIP treatment was done. The scratched area was monitored and snapped at 0, 24, and 48 h using an inverted microscope (Olympus, Japan). The wound area was analyzed through Image J software (NIH, USA) and a graph was plotted using GraphPad Prism 5.0 software (USA) (Tripathi and Biswal 2018).

Invasion assay

Briefly, control and PIP treated cells at 48 h were harvested and was reseeded on the upper chamber of matrigel

(Sigma-Aldrich, USA) pre-coated transwell chambers (Hi-Media Laboratories, India). The bottom chamber of the transwell inserts was augmented with serum (10% FBS) containing medium and cells were allowed to invade for 48 h. After that, non-invaded cells from the upper part were swiped out and the opposite side was fixed with methanol and stained with 1% crystal-violet (Tripathi and Biswal 2021). Three random places were selected, and manual enumeration and imaging of cells were done using an inverted microscope (Olympus, Japan).

Dual acridine orange/ethidium bromide fluorescent staining

Cells were seeded and treatment was given with desired concentrations of PIP for 48 h. Cells were harvested and stained with a mixture of dual stain: acridine orange (AO; 100 µg/ml) and ethidium bromide (EtBr; 100 µg/ml). Subsequently, imaging of stained cells was done using a fluorescence microscope (Olympus, Japan). Similarly, multicellular spheroids of A549 and NCI-H522 cells were exposed to desired concentrations of PIP for 48 h, stained with AO/EtBr and imaged (Tripathi et al. 2020).

Colony formation assay

Cells were seeded and then exposed to desired concentrations of PIP for 48 h. After treatment, the medium was replaced with a complete medium, and cells were allowed to develop into colonies for two weeks with a regular change of media after every 3 days. The experiment was terminated by fixing the colonies in 70% methanol, followed by staining with 0.1% crystal-violet and 1 × PBS wash to dry overnight (Tripathi et al. 2020). Colony images were captured using an inverted microscope (Olympus, Japan) and colonies with more than 50 cells were counted and plotted with the help of GraphPad Prism 5.0 software (USA).

Mitochondrial reactive oxygen species and superoxide measurement assay

PIP treated and untreated cells were collected in a centrifuge tube and mixed with 25 µM of 10,10'-Dimethyl-9,9'-biacridinium Bis(monomethyl Terephthalate) (MMT), and luminescence was measured in a luminometer. Further, cells were plated on a poly-L-lysine coated coverslip in a 6-well plate overnight and PIP treatment was done for 48 h. Then, MMT (25 µM) staining was done, and ROS production was analyzed and imaged under a confocal laser scanning microscope (CLSM) (Tripathi et al. 2020). However, for mitochondrial ROS analysis, PIP-treated lung cancer cells were stained with MMT for 25 min and analysis was done using a flow cytometer (BD Accuri™ C6, USA) Here, N-acetyl cysteine (NAC) was used as a positive control.

Measurement of mitochondrial membrane potential (MMP)

For fluorescence microscopic analysis of MMP, 24 h PIP-treated cells were fixed with ethanol and stained with rhodamine-123 followed by 1X PBS wash and imaged using a fluorescence microscope (Olympus, Japan). Additionally, MMP of PIP treated and untreated cells were analyzed using flow cytometry. In support of MMP reducing potential of PIP a positive control carbonyl cyanide m-chlorophenyl hydrazone (CCCP) (MMP alleviating agent) was used (Tripathi et al. 2020).

DAPI staining

Cells were treated with desired concentrations of PIP for 48 h and fixed using 4% PFA and stained with DAPI (1 µg/ml) in the dark. Then, cell imaging was done under a fluorescence microscope (Olympus, Japan) (Tripathi et al. 2020).

Comet assay

Briefly, PIP-treated, and untreated cells were harvested and mixed in low-melting agarose, pipetted over the slides (pre-coated with 1% normal melting agarose) and incubated in lysis buffer for 4 h at 4 °C in the dark. Post-lysis electrolysis was done in pre-cooled electrophoresis buffer at 0.74 V/cm for 30 min, followed by EtBr staining. About 25 comets were imaged under a fluorescence microscope (Olympus, Japan) and analyzed as per tail moment (head/tail DNA ratio) using CASP software (Collins et al. 2023).

Cell cycle arrest assay

Cells were incubated overnight to generate a confluent monolayer and treated with desired concentrations of PIP for 48 h. Cells were harvested, washed (in ice-cold 1X PBS), and fixed with ice-cold 70% alcohol. Fixed, treated, and untreated cells were further incubated in Triton X-100 and ribonuclease-A, and were washed with 1 X PBS. Additionally, cells were mixed with 50 µl propidium iodide (PI) (50 µg/ml) stain and cell cycle distribution was measured using a flow cytometer (BD Accuri™ C6, USA) (Tripathi and Biswal 2018).

Western blotting

Total protein extraction was done using lysis buffer and estimated through BCA protein assay kit. Thereafter, extracted proteins were resolved by performing SDS-PAGE gel electrophoresis and further transferred to cellulose nitrate transfer (blotting) membrane. The following primary antibodies are used in the study at manufacturer-recommended dilutions: E-cadherin, N-Cadherin, vimentin, slug, snail, claudin-1, β-catenin, SOX9, CD44, CD133, cleaved-PARP, cyclin-D1, and HRP conjugated secondary antibody (anti-rabbit) were procured from Cell Signaling Technology (Danvers, USA). Antibodies, such as Bcl-2, Bax, and β-actin, were procured from Santa Cruz Biotechnology, Inc. (Dallas, USA). Antibodies, such as caspase-9, cleaved-caspase-3, and HRP conjugated secondary (anti-mouse; 11–301), were purchased from ABGENEX (India). The protocol was followed from our previous published paper (Tripathi et al. 2020).

Tumorosphere formation

Cells were seeded in 2% w/v low melting agarose pre-coated 96-well plate and allowed to grow for three days to form multicellular spheroids. Spheroids were exposed to desired concentrations of PIP for 72 h. Spheres were analyzed and snapped at 0, 24, 48, and 72 h of PIP treatment using an inverted microscope (Olympus, Japan). Further, size (area; μm^2) was quantified in Image J software, and a graph was plotted through GraphPad Prism 5.0 software (USA). MTT assay and AO/EtBr staining were performed in control and PIP treated spheroids post 72 h treatment as described in Sect. 2.3 and 2.6, respectively (Tripathi and Biswal 2021).

Transient cell transfection

Briefly, A549 in the exponential growth phase were seeded in 6, 24, and 96-well culture plates and were allowed to grow overnight in a CO_2 incubator at 37 °C. Thereafter, cells were transfected with the mixture scramble or small-interfering RNA of SOX9 (siSOX9; Qiagen, India) prepared in lipofectamine-3000 reagent (Thermo-Fisher Scientific, USA) according to the manufacturer's instructions. Inhibition of SOX9 at protein level was confirmed by western blotting after 48 h of post-transfection (Tripathi and Biswal 2021).

Statistical analysis

The study used Graph-Pad Prism 5.0 software (USA) for all statistical analyses. Data showing P values < 0.05 were found statistically significant and significance levels between variables were done through a 2-tailed student's t-test. Probability (p) values ns = > 0.05, ***$p < 0.001$, **$p < 0.01$; *$p < 0.05$. The standard deviation (SD) signified the error bars, as mean ± SD of three independent experiments.

Results

Piperlongumine attenuates proliferation and single-cell colony-forming ability of human lung cancer cells

Initially, the potential of PIP (Fig. 1A) on viability and proliferation of human lung cancer cells A549 and NCI-H522 were evaluated by cell viability and single-cell colony formation assays, respectively. The cell viability assay results revealed that treatment concentration of PIP up to 6 µM did not show a significant reduction in the cell viability of, normal human epithelial cell line, HaCaT (Fig. 1B), while treatment of PIP up to 6 µM significantly reduced the cell viability of A549 and NCI-H522 cells at treatment time points 24, 48, and 72 h (Fig. 1C and D). The cytotoxicity assay data revealed that the IC_{50} of PIP for HaCaT, A549, and NCI-H522 cells were 7.5 µM, 5.35 µM, and 3.25 µM, respectively at 48 h of treatment. Interestingly, NCI-H522 cells exhibited more sensitivity towards PIP treatment than A549 cells. Thus, non-cytotoxic concentrations of PIP towards normal cells (up to 6 µM) were selected as treatment concentrations in A549 and NCI-H522 cells for further experiments. Further, PIP abrogated the colonization potential of A549 and NCI-H522 cells in concentration-dependent manner (Fig. 1E-G). As shown in Fig. 1E-G, A549 and NCI-H522 cells showed limited colonies at higher treatment concentrations of PIP. In essence, PIP reduces cell viability and growth rate of lung cancer cells relative to that of HaCaT.

Piperlongumine stimulates cell apoptosis in lung cancer cells

The apoptosis-inducing potential of PIP was checked in the lung cancer cells. As shown in Fig. 2A, DAPI staining revealed bright blue-fluorescent dots (chromatin condensation) in the center of PIP-treated A549 and NCI-H522 cells with respect to their parental control cells, which were significantly increased with increasing concentration of PIP. Consistent with the previous findings, AO/EtBr staining results suggested the induction of apoptosis in PIP-treated A549 and NCI-H522 cells (Fig. 2B and C). AO/EtBr staining of PIP-treated A549 and NCI-H522 cells displayed bright green dots, orange-nuclear dots, and red-stained cells with respect

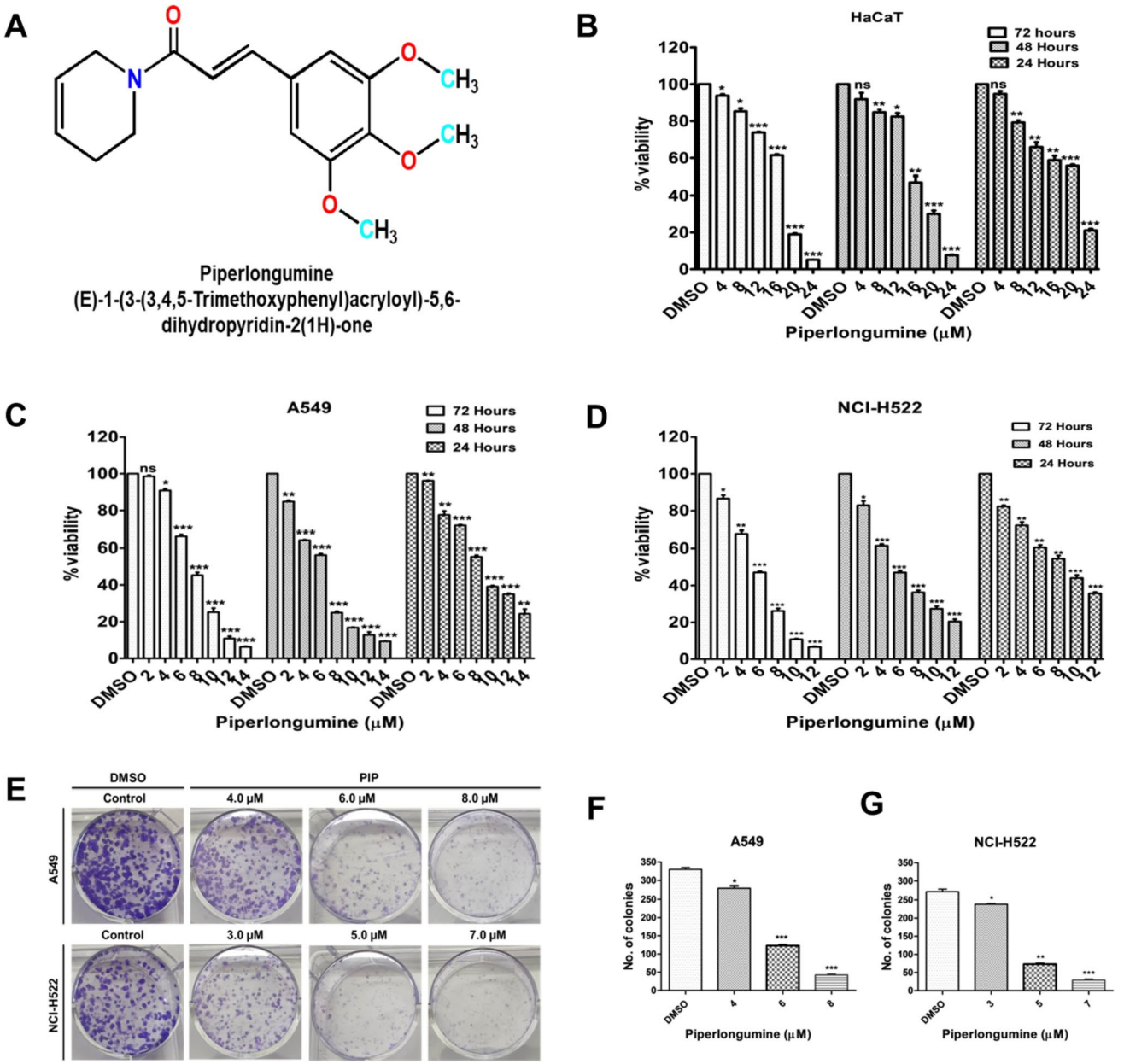

Fig. 1 Piperlongumine shows selective cytotoxicity and anti-proliferative activity towards lung cancer cells. **A** The chemical structure of phytochemical piperlongumine (PIP). **B**–**D** The histogram showed the cell viability of HaCaT, A549, and NCI-H522 cells after treatment with desired concentrations of PIP (0–24 μM) for 72, 48, and 24 h. **E** Crystal violet staining data showed PIP (0–8 μM) effectively suppressed the single-cell colony-forming potential of A549 and NCI-H522 cells in a concentration-dependent manner. **F**, **G** The histograms showed quantitative data of the number of colonies growing in control and PIP treated A549 and NCI-H522 cells

to their uniformly green-stained untreated control cells indicating early apoptosis, late apoptosis, and necrosis, respectively (Fig. 2B and C). Mechanistically, PIP treatment stimulated the activation of the caspase-dependent apoptotic pathway. It was observed that PIP-treated A549 cells showed high expression of Bax, cleaved PARP, caspase-9, and cleaved-caspase-3 while reduced expression of Bcl-2 (Fig. 2D-I). Taken together, it could be concluded that PIP persuades apoptosis in lung cancer cells via caspase-dependent apoptotic pathway.

Piperlongumine induces DNA damage and cell cycle arrest in lung cancer cells

To further explore the mechanism of the apoptosis and anti-proliferative potential of PIP, comet assay and cell

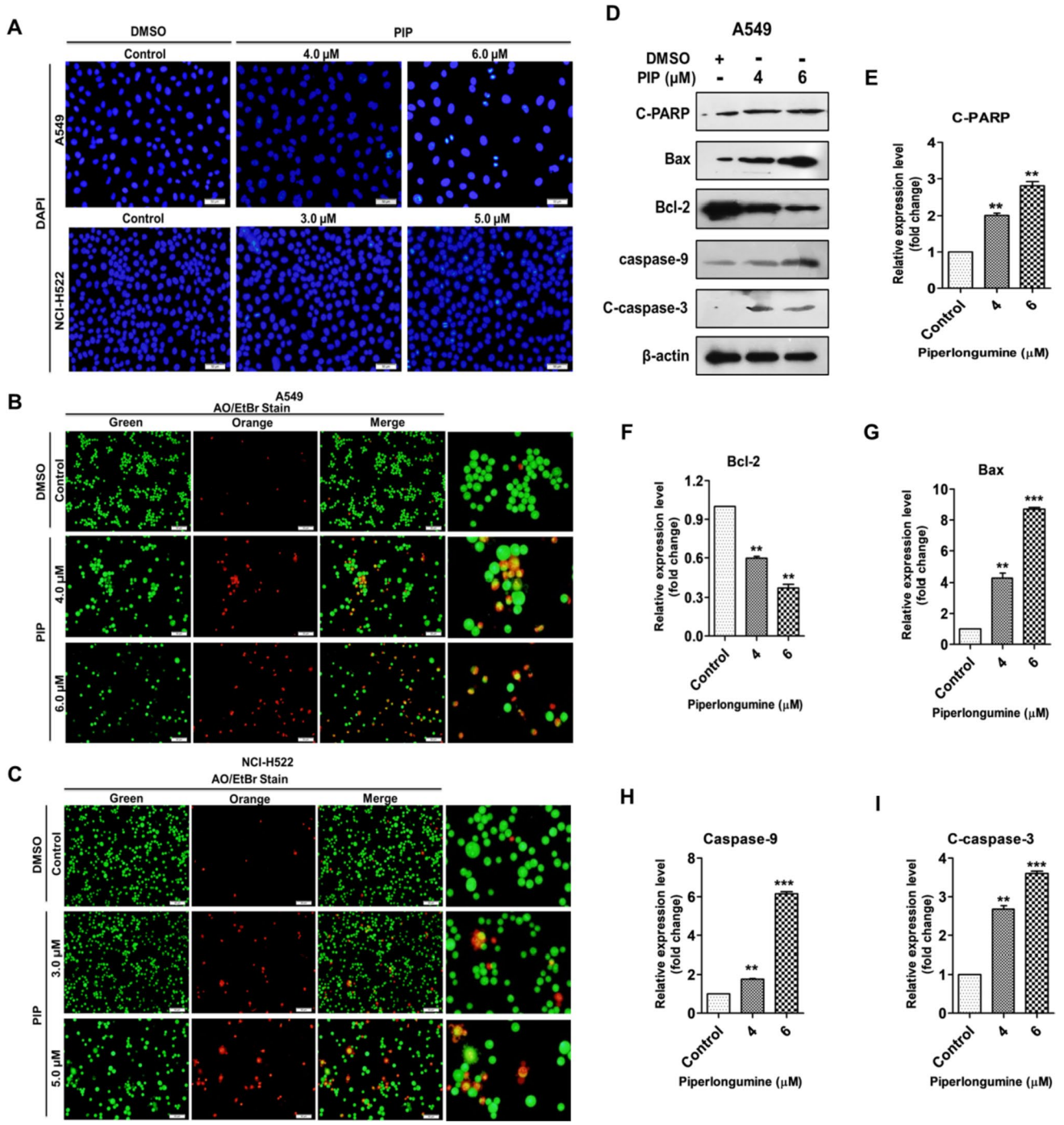

Fig. 2 Piperlongumine promotes chromatin condensation and caspase-dependent apoptosis in lung cancer cells. **A** DAPI staining showed nuclear morphological changes in A549 and NCI-H522 cells after 48 h treatment of PIP. **B**, **C** AO/EtBr staining showed cellular morphological changes (apoptosis induction) in A549 and NCI-H522 cells after 48 h treatment of PIP. **D** Western blot data of control and PIP-treated A549 cells showed relative expression levels of pro-apoptotic, anti-apoptotic, and caspase-dependent apoptotic proteins. **E–I** Quantitative data showed relative expression levels of pro-apoptotic, anti-apoptotic, and caspase-dependent apoptotic proteins in control and PIP-treated A549 cells. β-actin represents loading control

cycle distribution were evaluated. Comet cells analysis showed a significant increase in the tail moment in PIP-treated A549 and NCI-H522 cells compared with control cells in a concentration-dependent manner (Fig. 3A-C). Furthermore, flow cytometry analysis shows that treatment with a higher concentration of PIP effectively arrested the

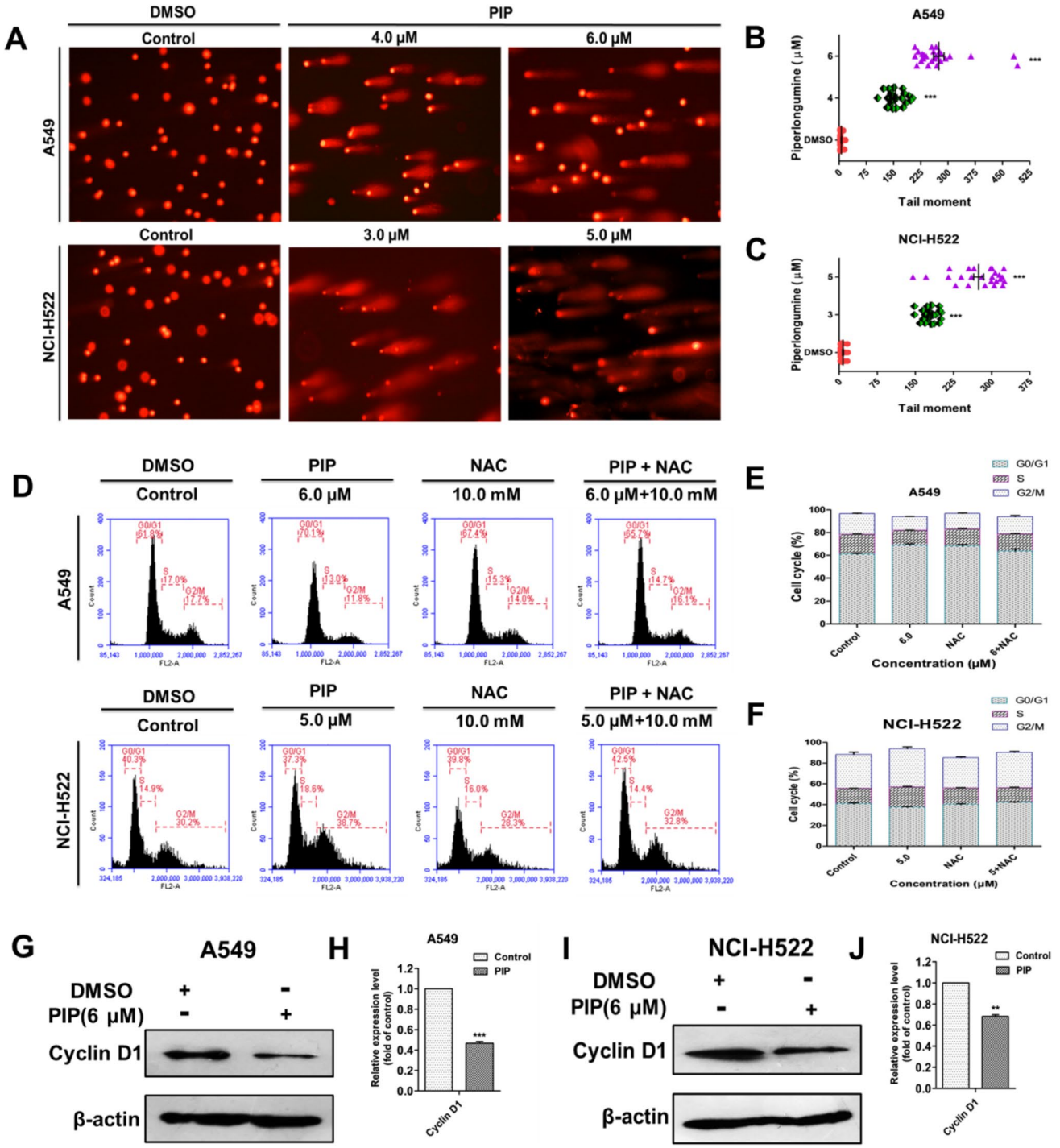

Fig. 3 Piperlongumine induces DNA damage and cell cycle arrest in lung cancer cells. **A** Comet assay data of A549 and NCI-H522 cells after treatment with PIP at 24 h using EtBr stain. **B**, **C** The histograms showed quantitative data of DNA tail length in control and PIP-treated A549 and NCI-H522 cells, exacerbated in a concentration-dependent manner. **D** Cell cycle distribution in control, PIP, NAC, and PIP + NAC treated A549 and NCI-H522 cells using PI stain. **E**, **F** The histograms showed G1, S, and G2/M phase distribution in control, PIP, NAC, and PIP + NAC treated A549 and NCI-H522 cells. **G**–**J** Western blotting data showed the treatment effect of PIP on the expression of cell cycle regulatory protein cyclin D1 for 48 h. β-actin represents loading control

A549 and NCI-H522 cells in G0/G1 phase and S-G2/M phase, respectively (Fig. 3D). It was observed that treatment of A549 cells with a higher concentration of PIP (6 μM) for 24 h increased the proportion of G0/G1 phase (70.1%) as compared with control cells (61.8%) (Fig. 3E). Moreover, treatment of NCI-H522 cells with a higher

concentration of PIP (5 µM) for 24 h increased the proportion of S-G2/M phase (18.6–38.7%) as compared with control cells (14.9–30.2%) (Fig. 3F). Interestingly, treatment of a well-known ROS scavenger, NAC with a combination of PIP in A549 and NCI-H522 cells drastically reversed the cell cycle arrest potential of PIP (Fig. 3D-F). In addition, PIP also downregulated the expression of regulatory subunit protein of cyclin-dependent kinases, cyclin D1 in A549 and NCI-H522 cells at higher treatment concentrations (Fig. 3G–J). In essence, these findings suggested that PIP obstructs lung cancer cell proliferation via ROS-mediated cell cycle arrest.

Piperlongumine promotes cellular and mitochondrial reactive oxygen species generation and alleviation in mitochondrial membrane potential of lung cancer cells

We preliminarily reconnoitred that anti-proliferation and cell cycle arrest with PIP exposure was mediated by ROS. Thus, we investigated the effect of PIP on intracellular and intra-mitochondrial ROS levels in lung cancer cells. At first, intracellular superoxide investigation using a luminometer showed enhanced chemiluminescence in PIP-treated A549 and NCI-H522 cells as compared with control cells in a

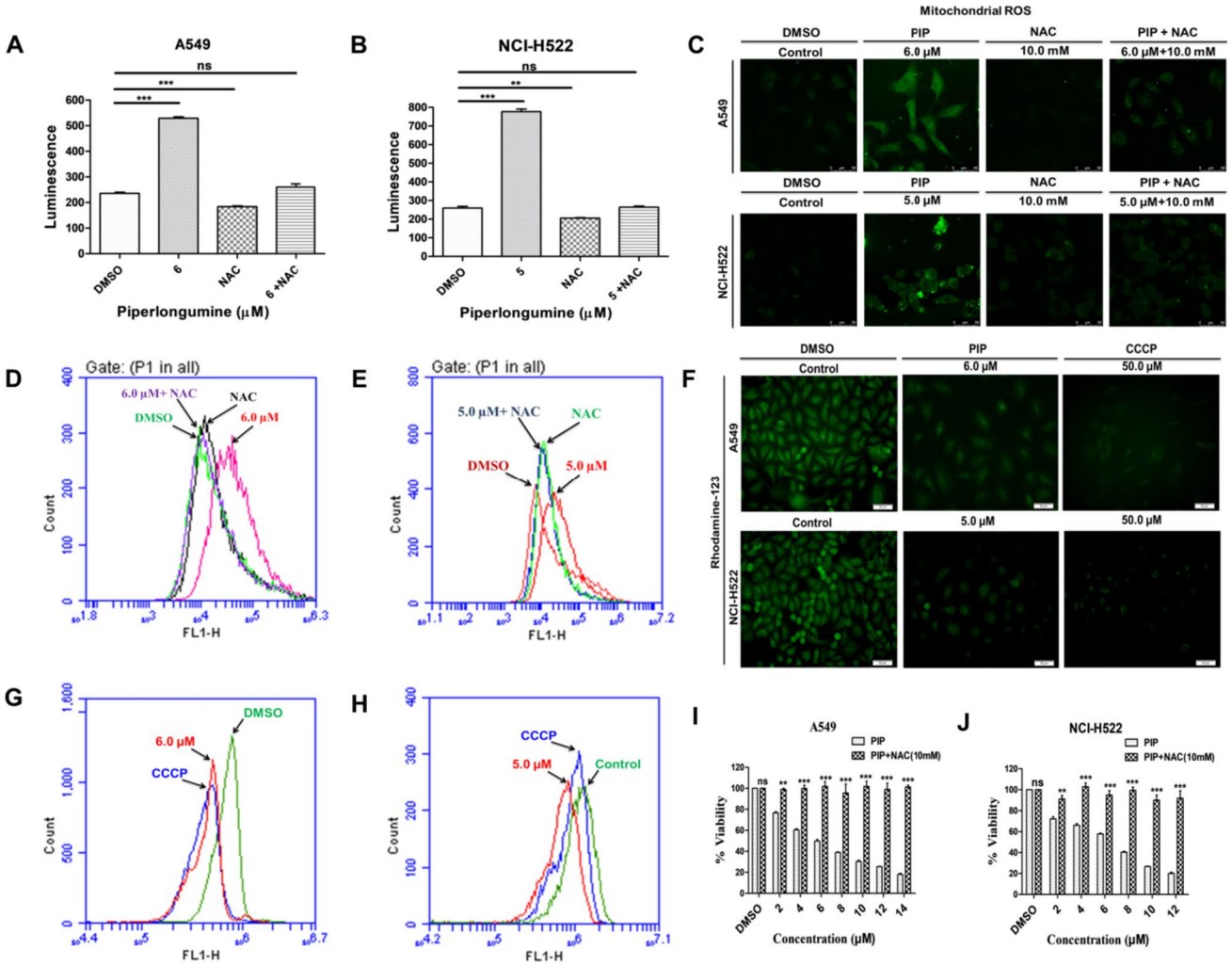

Fig. 4 Piperlongumine induces cellular and mitochondrial ROS dysregulates MMP leads to cytotoxicity on lung cancer cells. **A**, **B** The graph showed quantitative data of cellular ROS levels in control, PIP, NAC, and PIP with NAC treated lung cancer cells for 12 h. **C** The CLSM data showed sub-cellular (mitochondrion) ROS levels in control, PIP, NAC, and PIP with NAC treated lung cancer cells for 12 h. **D**, **E** Flow cytometry analysis showed sub-cellular (mitochondrion) ROS levels in control, PIP, NAC, and PIP with NAC treated lung cancer cells **D** A549 **E** NCI-H522, for 12 h. **F** Rhodamine-123 stained A549 and NCI-H522 cells showed reduced mitochondrial membrane potential after 24 h of PIP and CCCP (positive control) treatment through fluorescence microscopy analysis. **G**, **H** Rhodamine-123 stained **G** A549 and **H** NCI-H522 cells showed reduced mitochondrial membrane potential after 24 h of PIP and CCCP (positive control) treatment through flow cytometry analysis. **I**, **J** The histograms showed PIP-induced ROS-mediated cytotoxicity in lung cancer cells

concentration-dependent manner (Fig. 4A-B). However, chemiluminescence was effectively suppressed in a combination of ROS antagonist (NAC) and PIP treated A549 and NCI-H522 cells, indicating intracellular superoxide promoting potential of PIP (Fig. 4A-B). Next, subcellular (mitochondria) ROS production was checked through confocal microscopy and flow cytometry. Results of confocal microscopy showed an effective increase in green fluorescence in PIP-treated A549 and NCI-H522 cells, indicating enhanced mitochondrial ROS level as compared with control (Fig. 4C). However, treatment of cells with the combination of ROS antagonist (NAC) and PIP caused a surprising decrease in green fluorescence, indicating mitochondrial ROS enhancing the potential of PIP (Fig. 4C). The result was further confirmed by finding the right shift in the peak of PIP treated A549 and NCI-H522 cells than their respective control cells via flow cytometry (Fig. 4D and E). Besides, the shifting of peaks in NAC alone or in combination with PIP-treated A549 and NCI-H522 towards the left as compared with their respective control cells confirmed the mitochondrial ROS enhancing the potential of PIP (Fig. 4D and E). Dysregulated mitochondrial membrane potential (MMP) can play a very effective role in mitochondrial-mediated cell death of human cancer cells. Overproduction of ROS can oxidize the pores of the mitochondrial membrane which may dysregulate the MMP of cancer cells. Thus, fluorescence microscopy study involving Rhodamine-123 dye showed an effective decrease in green fluorescence in PIP and CCCP (50 µM) treated A549 and NCI-H522 cells, indicating a loss in MMP as compared with untreated control (Fig. 4F). Additionally, shift in the peaks of PIP and CCCP treated A549 and NCI-H522 cells towards the left as compared with their respective untreated control peaks were observed, which confirmed the striking MMP reducing the potential of PIP (Fig. 4G and H). PIP-mediated upsurge in mitochondrial ROS promoted depletion in MMP followed by enhanced permeability of mitochondria membrane, which leads to higher ROS in a cell system. Thus, cell viability assay was further performed to investigate the influence of ROS on the cytotoxic potential of PIP in A549 and NCI-H522 cells. NAC in combination with PIP effectively inhibited the cytotoxicity of PIP on A549 and NCI-H522 cells, establishing a functional relationship between the cytotoxic potential of PIP and ROS (Fig. 4I and J). Taken together, this finding denotes that PIP induces ROS-mediated cytotoxicity in lung cancer cells.

Piperlongumine disrupts the cytoskeletal organizations and impedes the growth of lung cancer cells

Invasion and migration are the key hallmarks of tumor malignancy that implies invasive and migratory behavior of cells through cytoskeletal organization F-actin filament. Thus, morphological changes in F-actin filament using Alexa Fluor 488 phalloidin stain results that PIP treatment disrupted the elongated projections and polygonal shapes (actin filament) of A549 and NCI-H522 cells, which were visible in untreated control cells (Fig. 5A and B). To further validate the potential of PIP on cell migration and invasion, wound healing and the transwell invasion assays were performed. PIP treatment effectively retarded the migration and wound-closer rate of A549 and NCI-H522 cells from the edge of the wound towards the center as compared with control cells (Fig. 5C–F). Additionally, PIP also inhibited the invasion rate of A549 and NCI-H522 cells as compared with control cells (Fig. 5G–I). In essence, these results suggest that PIP potentially suppresses the invasion and migration potential of lung cancer cells.

Piperlongumine inhibits the epithelial to mesenchymal transition and stem-cell phenotype of lung cancer cells

EMT implies promoting the invasion and migration of cancer cells. Initially, immunocytochemistry (ICC) analysis data suggested that treatment of PIP in A549 cells effectively increased the expression of epithelial marker protein E-cadherin and suppressed the expression of mesenchymal marker protein vimentin in a concentration-dependent manner (Fig. 6A and B). Furthermore, the data of ICC was further validated by examining the effect of PIP treatment on the expression of EMT marker proteins through western blot assay. Western blot data also suggested that PIP treatment effectively enhanced the expression of E-cadherin and suppressed the expression of vimentin in A549 and NCI-H522 cells (Fig. 6C–F). Additionally, PIP suppressed the expression of few other mesenchymal markers, such as β-catenin, claudin-1, N-cadherin, slug, snail, and vimentin in A549 and NCI-H522 cells (Fig. 6C–F). Furthermore, treatment of A549 and NCI-H522 cells with PIP showed an effective decrease in the expression of stem-cell marker proteins, such as SOX9, CD133, and CD44 (Fig. 6G–J). Together, these findings denote that PIP potentially obstructed the EMT and stemness in lung cancer cells.

Piperlongumine inhibits tumorigenesis at higher treatment concentrations ex vivo

Multicellular spheroids show very much resemblance to solid tumor microenvironment in cell appearance, growth, and proliferation. Therefore, multicellular spheroids can be used for the screening of newer anticancer compounds as a promising model system ex vivo. Lower concentrations of PIP treatment did not show very effective results on multicellular spheroids that might be due to in vivo tumor microenvironment-like conditions. At first, multicellular spheroids were developed ex vivo and equal size of spheroids was selected for the study. Post-treatment

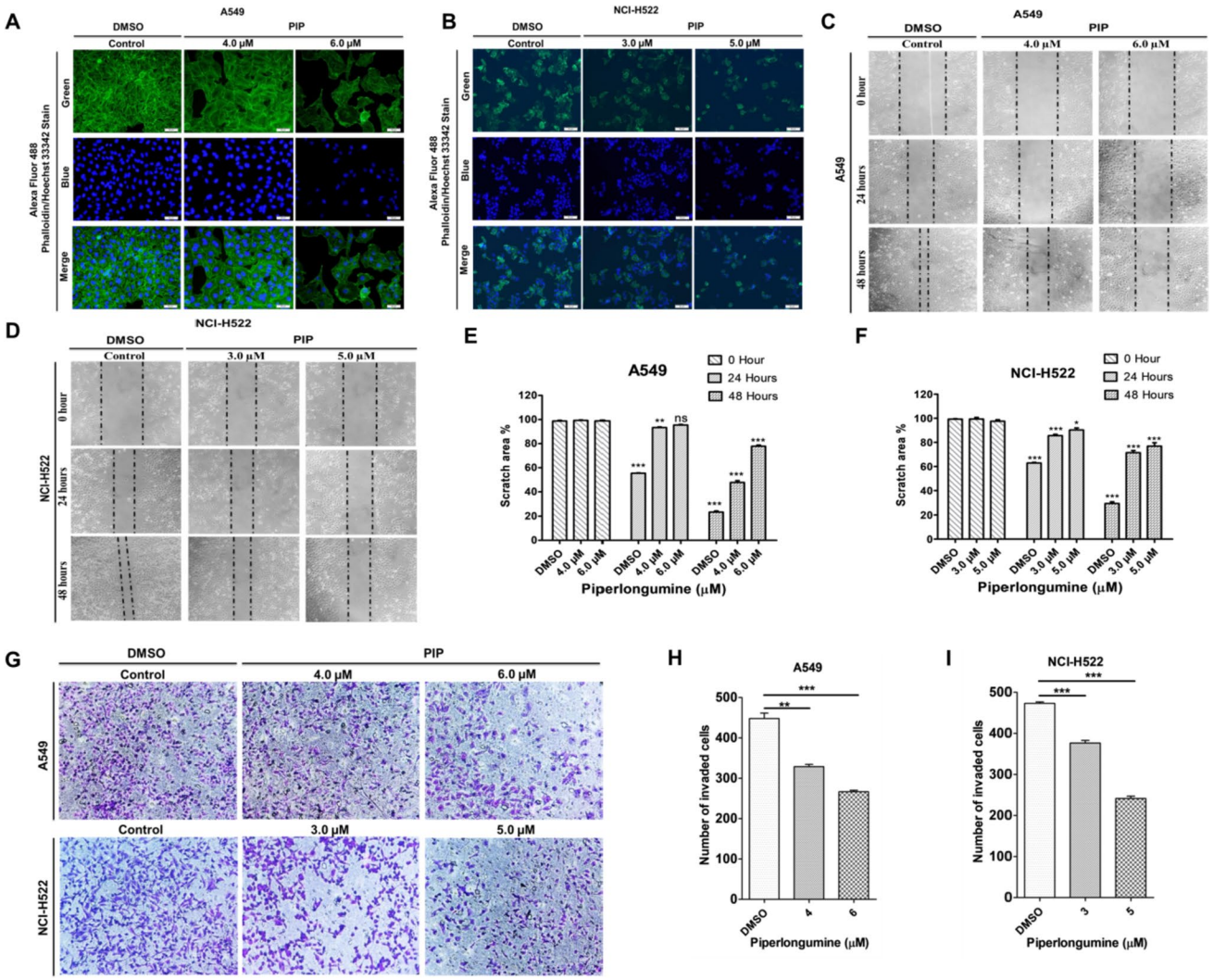

Fig. 5 Piperlongumine disrupts cytoskeletal morphology and inhibits the spread of lung cancer cells. **A**, **B** Immunofluorescence assay data showed morphological disruption of F-actin filament in PIP-treated A549 and NCI-H522 cells as compared with control cells in a concentration-dependent manner. **C**, **D** Wound healing migration assay data showed an effective diminution in migration rate of PIP-treated A549 and NCI-H522 cells as compared with control cells in a concentration-dependent manner. **E**, **F** The histograms showed quantitative data of reduction in migration rate of PIP-treated A549 and NCI-H522 cells as compared with control cells in a concentration-dependent manner. **G** Invasion assay data showed an effective diminution in invasion rate of PIP-treated A549 and NCI-H522 cells as compared with control cells in a concentration-dependent manner. **H**, **I** The graph showed quantitative data of effective reduction in the invasion rate of PIP-treated A549 and NCI-H522 cells as compared with control cells in a concentration-dependent manner

with desired concentrations of PIP effectively abridged the size and surface area of multicellular spheroids of A549 and NCI-H522 cells (Fig. 7A–D). Furthermore, AO/EtBr staining of multicellular spheroids revealed that PIP-treated multicellular spheroids were stained more with EtBr than AO (Fig. 7E and F). In contrast, control multicellular spheroids were stained more with AO than EtBr (Fig. 7E and F). This finding suggested that PIP treatment induced apoptosis in multicellular spheroids in a concentration-dependent manner. Analysis through cell viability assay further confirmed that PIP-treated multicellular spheroids contain less viable cells than untreated control multicellular spheroids (Fig. 7G and H). Taken together, it could be concluded that PIP inhibits tumorigenesis at higher treatment concentrations ex vivo.

Piperlongumine induces more potent cytotoxicity and inhibits proliferation, invasion, and migration in SOX9 knockdown lung cancer cells

One of our recent articles documented that SOX9 promotes lung cancer drug resistance via enhancing cell proliferation, invasion, and migration (Tripathi and Biswal 2021). However, the knockdown of SOX9 reversed the effect. Thus,

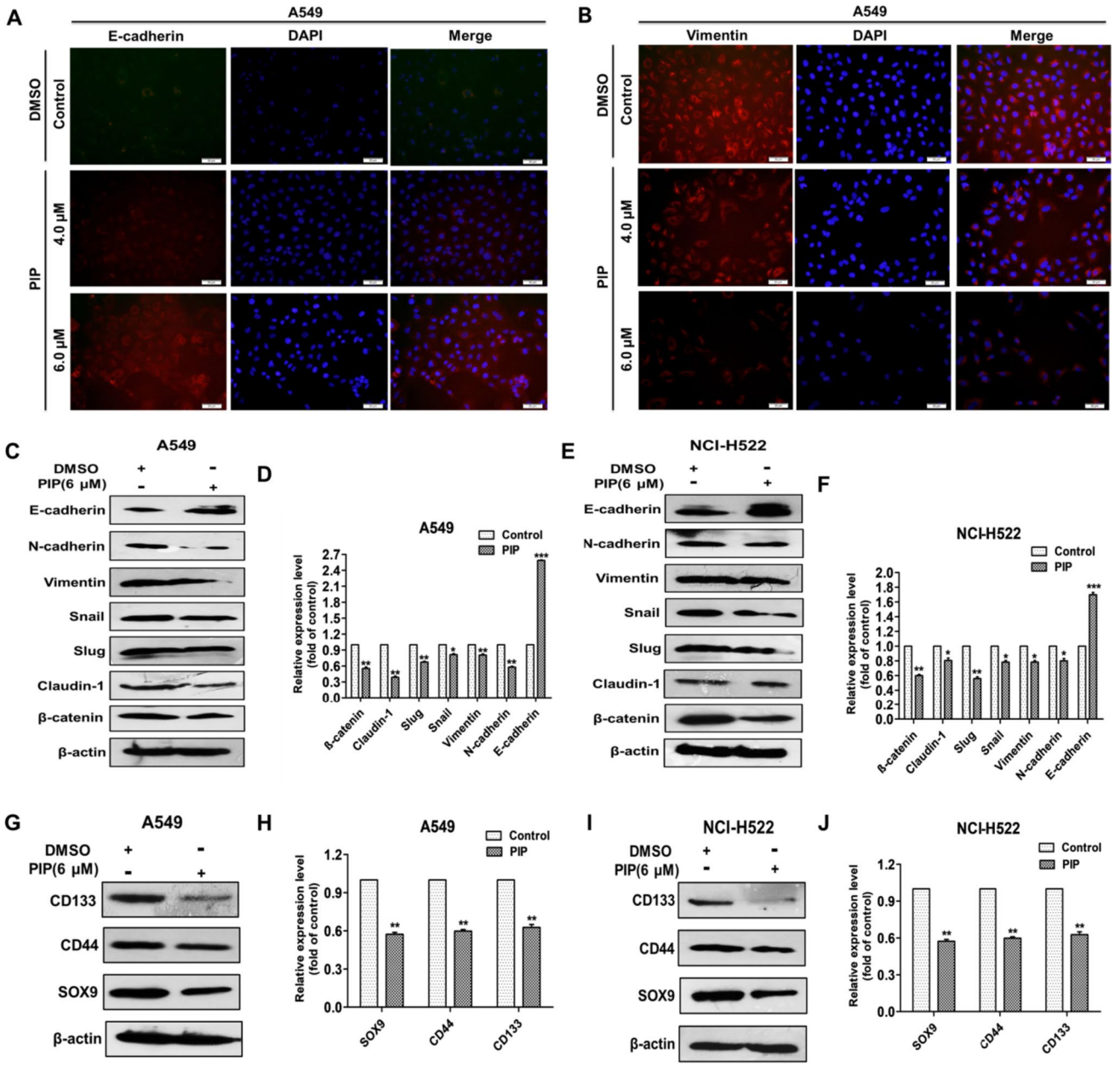

Fig. 6 Piperlongumine modulates the expression of EMT and stemness markers in lung cancer cells. **A**, **B** Immunocytochemistry data showed an effective upsurge in E-cadherin and diminution in vimentin at protein levels in PIP-treated A549 cells than control cells. **C**, **E** Western blot data showed upregulation of epithelial and diminution of mesenchymal markers in PIP-treated A549 and NCI-H522 cells. **D**, **F** The histograms showed quantitative data of changes in the expression of EMT marker proteins in A549 and NCI-H522 cells after treatment with PIP for 48 h. **G**, **I** Western blot data showed an effective diminution in the expression of stemness marker proteins in PIP-treated A549 and NCI-H522 cells. **H**, **J** The histograms showed quantitative data of changes in the expression of stemness marker proteins in A549 and NCI-H522 cells after treatment with PIP

the mechanism of the anti-lung cancer potential of PIP was examined in transient SOX9 knockdown lung cancer cell line. At first, lung cancer cell line, A549, was transiently transfected with siSOX9, and silencing of SOX9 was confirmed through western blotting (Fig. 8A and B). Furthermore, Fig. 8C showed that PIP treatment significantly reduced the cell viability of siSOX9 transfected A549 cells than PIP alone treated or only siSOX9 transfected A549 cells. Additionally, PIP treatment in siSOX9 transfected A549 cells effectively inhibited their migration and invasion rate as compared with PIP alone treated or only siSOX9 transfected A549 cells (Fig. 8D–G). Taken together, it can

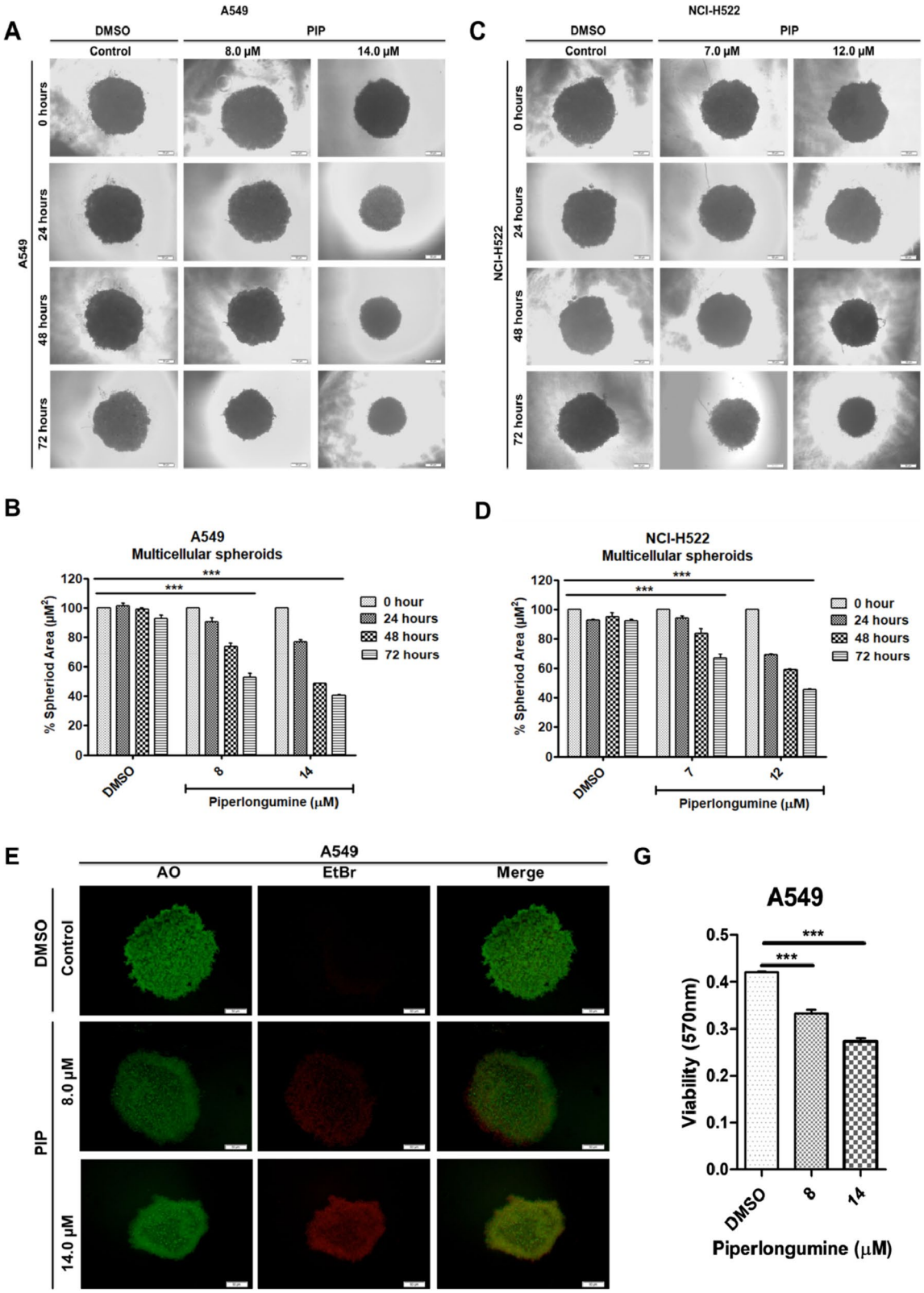

Fig. 7 Piperlongumine inhibits growth and induces cytotoxicity and apoptosis in multicellular spheroids of lung cancer cells. **A**–**D** PIP treatment effectively reduced the size of multicellular spheroids of A549 and NCI-H522 cells in a concentration and time-dependent manner. **E**, **F** AO/EtBr staining of multicellular tumor spheroids of A549 and NCI-H522 cells treated with different concentrations of PIP for 72 h showed a positive correlation between apoptosis rate and increasing concentration of PIP. **G**, **H** The graph showed PIP-induced cytotoxicity on multicellular tumor spheroids of A549 and NCI-H522 cells at 72 h of treatment by MTT assay

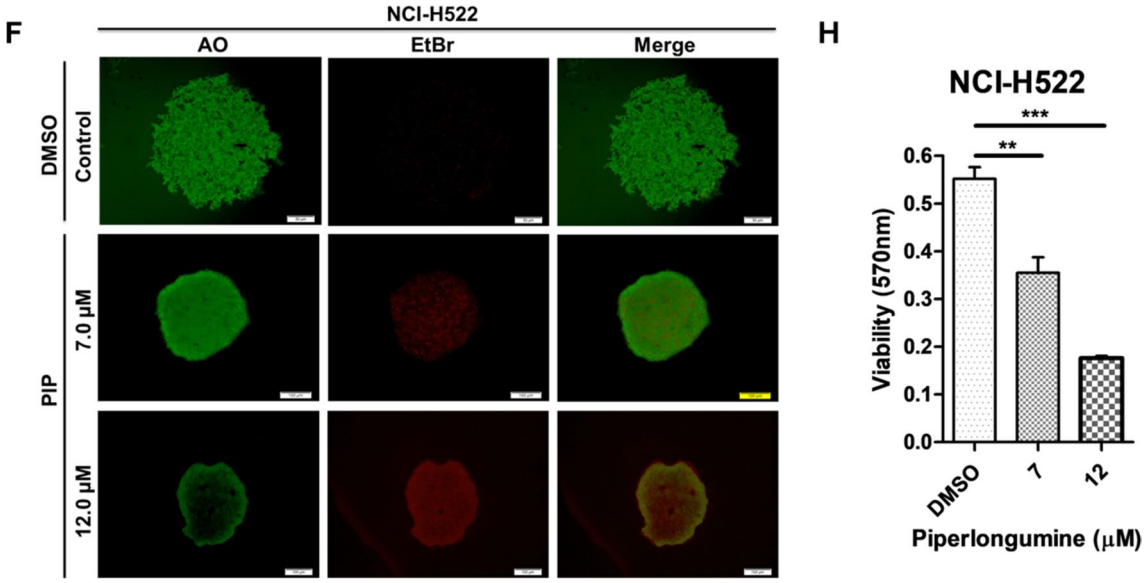

Fig. 7 (continued)

be concluded that expression of SOX9 supports in viability, invasion, and migration in lung cancer. However, PIP showed more potent cytotoxicity, anti-invasive, and anti-migration activities in SOX9 knockdown lung cancer.

Discussion

Currently, phyto-based compounds have gained enormous research attention due to their extensive medicinal values including selective anticancer effects at a significantly lower dose with limited toxicity (Tripathi et al. 2019). PIP, an active alkaloid/amide, has been well recognized for its antitumor potential against many malignant tumors (Tripathi and Biswal 2020). Herein, we first contemplate the molecular mechanism of the anticancer potential of PIP in lung carcinoma through deterring EMT and stemness. Our results indicate that PIP exerts significant growth inhibition with appreciable cytotoxicity on lung cancer cells. NCI-H522 cells were detected more sensitive towards PIP exposure than A549 cells. Recent study has reported that phyto-compound significantly inhibit rapid proliferation and colonization of cancer cells at lower concentration (Tripathi et al. 2020). Relatively, we found that PIP effectively inhibits the single-cell colony-forming potential of lung cancer cells, strongly supporting its anti-proliferative and anti-colonizing potential. Apoptosis is a well-controlled biological mechanism induced by anticancer drugs via activation of multiple pathways including the caspase-dependent apoptotic pathway (Rajabi et al. 2021). DAPI and dual AO/EtBr staining results suggest the observed effect of nuclear condensation and morphological changes semblance with early apoptosis, late apoptosis, and necrosis after PIP exposure in lung cancer cells. A previous study has shown that PIP-induced caspase-based apoptosis in triple-negative breast cancer cells by inhibiting PI3K/Akt/mTOR pathway (Shrivastava et al. 2014). Similarly, we found that PIP promotes apoptosis in lung cancer cells through upregulating pro-apoptotic protein Bax, activating caspase-dependent apoptotic pathway proteins, like cleaved caspase-3/9 and downregulating anti-apoptotic protein Bcl-2. Apart from apoptosis, DNA damage and cell cycle arrest are some other imperative mechanisms induced by various anticancer drugs to inhibit cancer cell proliferation leading to cell death (Carlos et al. 2020). Our findings revealed that PIP induced DNA damaging effects and cell cycle arrest in lung cancer cells. PIP significantly arrested the A549 cells in the G0/G1 phase and NCI-H522 cells in the S-G2/M phase of the cell cycle by inhibiting the expression of checkpoint protein cyclin D1. Various anticancer drugs are known to exert anticancer activity via stimulating excess cellular and subcellular ROS generation that may cause severe oxidative damage leading to cancer cell death (Chen et al. 2015). Similarly, our findings suggested that treatment of PIP with NAC attenuates the PIP-induced cell cycle arrest of lung cancer cells, indicating ROS-mediated anti-proliferative effect and cell cycle arrest. Previous studies have reported that excess ROS can disrupt the MMP that leads to mitochondrial dysfunction and finally cancer cell death (Pandey et al. 2020; Tripathi et al. 2020). The current study findings strongly support the cellular and mitochondrial ROS enhancing potential of PIP in lung cancer cells. Further, excessive accumulation of mitochondrial ROS triggers loss of MMP, suggesting ROS-induced mitochondrial damage is involved in the cytotoxic potential of PIP in lung

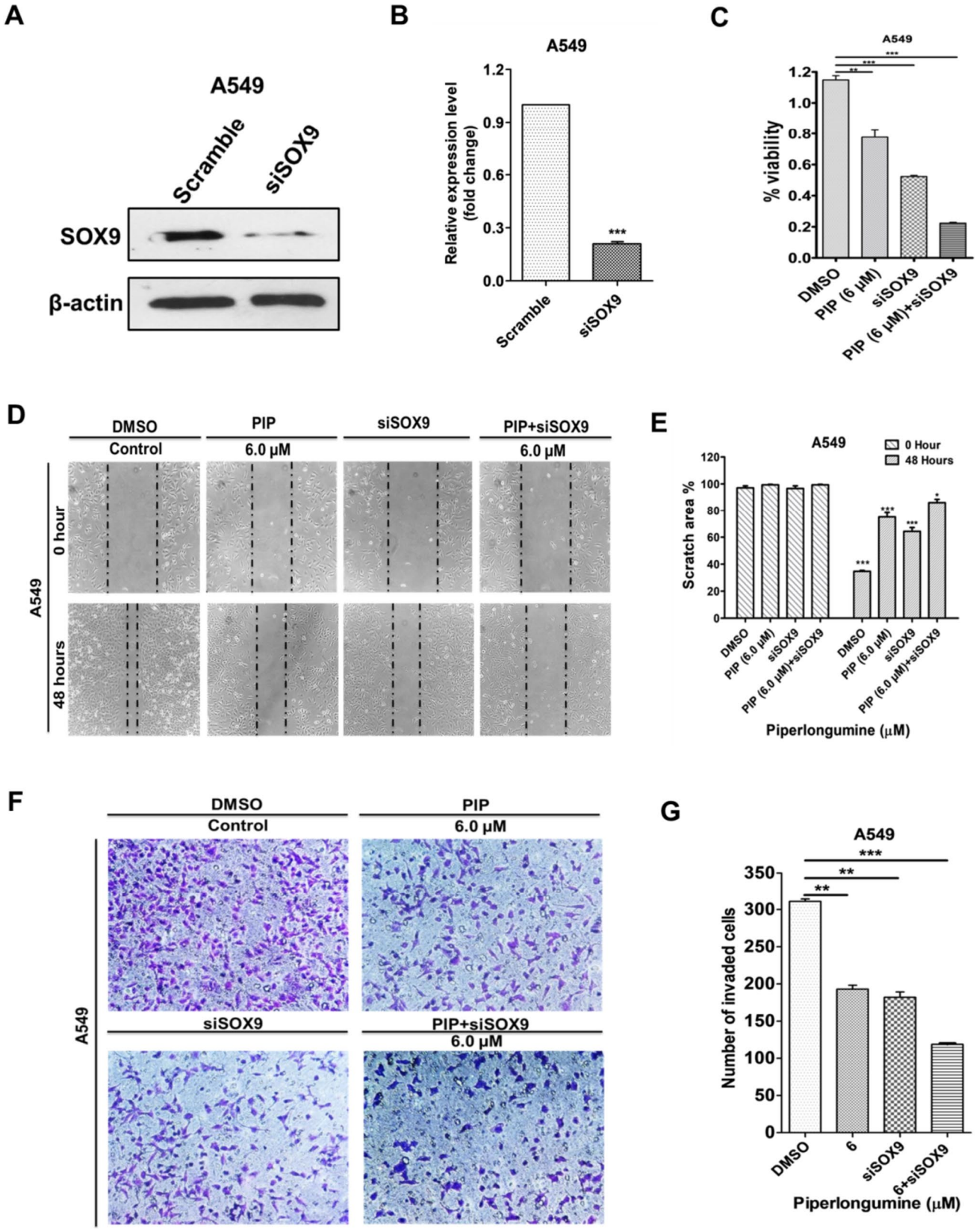
A
A549
Scramble
siSOX9
SOX9
β-actin
B
A549
Relative expression level (fold change)
1.2
0.9
0.6
0.3
0.0
***
Scramble
siSOX9
C
A549
***
***
**
% viability
1.2
1.0
0.8
0.6
0.4
0.2
0.0
DMSO
PIP (6 μM)
siSOX9
PIP (6 μM)+siSOX9
D
DMSO
Control
PIP
6.0 μM
siSOX9
PIP+siSOX9
6.0 μM
A549
0 hour
48 hours
E
A549
0 Hour
48 Hours
Scratch area %
120
100
80
60
40
20
0
***
***
***
*
DMSO
PIP (6.0 μM)
siSOX9
PIP (6.0 μM)+siSOX9
DMSO
PIP (6.0 μM)
siSOX9
PIP (6.0 μM)+siSOX9
Piperlongumine (μM)
F
DMSO
Control
PIP
6.0 μM
siSOX9
PIP+siSOX9
6.0 μM
A549
G
A549
***
**
**
Number of invaded cells
350
300
250
200
150
100
50
0
DMSO
6
siSOX9
6+siSOX9
Piperlongumine (μM)

◂**Fig. 8** Piperlongumine shows higher cytotoxicity and growth-inhibiting potential in SOX9 knockdown A549 cells. **A**, **B** The western blot assay data showed transient knockdown of SOX9 in lung cancer cell line, A549. **C** Cell viability assay data showed an effective increase in the cytotoxic potential of PIP in SOX9 knockdown A549 cells treated for 48 h through MTT assay. **D**, **E** The wound healing scratch assay data showed a potent increase in the anti-migratory potential of PIP in SOX9 knockdown A549 cells treated for 48 h. **F**, **G** The invasion assay data showed a potent increase in the anti-invasive potential of PIP in SOX9 knockdown A549 cells treated for 48 h

cancer cells. Thus, considering these findings, we can conclude our results that accumulation of mitochondrial ROS activates caspase-dependent apoptosis pathway in lung cancer cells. Deregulation of EMT pathway proteins implies to invasion and migration of solid malignant tumors (Dudás et al. 2020). However, reorganization of actin cytoskeleton promotes dynamic elongation, directional motility, and sheet-like membrane protrusions of cells, thereby invasion of cells (Lamouille et al. 2014; Liu et al. 2017). Various drugs have been known for their potential to inhibit the invasion and migration of tumor cells by targeting differentially expressed EMT markers (Otsuki et al. 2018; Dudás et al. 2020). The current study results revealed that PIP induces the dis-organization of elongated projections and polygonal shapes of F-actin cytoskeleton in lung cancer cells. Furthermore, disorganization of F-actin cytoskeleton attenuates invasion and migration of lung cancer cells through upregulating the epithelial marker E-cadherin and downregulating mesenchymal marker proteins, such as β-catenin, claudin-1, N-cadherin, slug, snail, and vimentin. Previous studies documented that the reorganization of actin cytoskeleton and acquisition of EMT phenotype promote stem-like traits, which favors primary tumors to become malignant and invasive (Haynes et al. 2011; Tripathi and Biswal 2021). The present study showed that PIP attenuates the expression of stem-cell marker proteins, such as SOX9, CD133, and CD44. Mechanistically, the study reported that expression of SOX9 favors the survival of lung cancer cells and PIP showed more potent cytotoxic, anti-proliferative, anti-invasive, and anti-migratory effects in SOX9 knockdown lung cancer cells. Studies evident that multicellular spheroid has indeed been semblance with in vivo tumor model in microenvironment, proliferation, and growth and are unlike too in vitro model (Li et al. 2021). Multicellular spheroids show resistance to most of the therapies, including chemo-, radio-, and phototherapy. Previous studies have shown that in case of human lung carcinoma (A549), cells in MCTs exhibited about 6600 times more resistance to vinblastine treatment than cells in monolayer (Han et al. 2021). Considering these facts, we used a higher dose of PIP for our ex vivo study and our results showed that PIP exerts a significant reduction in size and cell viability and induction of apoptosis in multicellular spheroids of lung cancer cells, suggesting a potent anti-tumorigenic effect. The efficiency of PIP can be increased by nano-encapsulation, which will allow it to penetrate in the ex vivo multicellular spheroids that can mimic tumor conditions. This encapsulation of PIP may target the core cells in the multicellular spheroids, where normal dosing was not reachable (Yasamineh et al. 2023). Lastly, our results strongly supported the anticancer potential of SOX9 in lung cancer cells via a precise molecular mechanism like modulation of EMT phenotype and stem-like traits.

Conclusion

Diagnosis of lung cancer remains exceedingly poor which pressing demand to search some novel compounds with potent anticancer activity. Herein, we demonstrate that PIP induces cytotoxicity and anti-proliferative activities through cell cycle arrest and activation of the caspase-dependent apoptotic pathway on lung cancer cells. Our results support that PIP induces apoptosis through elevating mitochondrial and cellular ROS and dissipating MMP, which damages the subcellular organelles and molecules, including mitochondria and DNA. Moreover, we also report that PIP is highly effective against the migratory and invasive nature of lung cancer cells by dis-organizing F-actin cytoskeleton leading to inhibition of EMT and stemness phenotype. Meanwhile, ex vivo anti-tumorigenic activity of PIP against multicellular spheroids of lung cancer is further reported first time. Our study first time demonstrates that PIP disorganize cytoskeleton and attenuates EMT and stemness markers, resulting lung cancer cell death. Thus, PIP might have emerged as a promising therapeutic agent in the treatment of lung cancer after rigorous drug development research and future clinical trials.

Authors contributions SKT and BKB designed the research. SKT conducted all the experiments and analyzed data. SKT and RKS prepared the manuscript. All authors read and approved the manuscript. The authors declare that all data were generated in-house and that no paper mill was used.

Funding This research work is supported by the project (Grant Number: ECR/2016/000792) under the Department of Science and Technology, Science and Engineering Research Board (DST, SERB), New Delhi, India, and Department of Science and Technology, Odisha, India, (Grant no-1201).

Data availability The data that support the findings of this study are available on request from the corresponding author.

Declarations

Ethical approval As the in vitro experiments were performed on cell lines, approval from the ethics committee was not required for this study.

Competing interests The authors declare no competing interests.

References

Alagheband Y, Jafari-gharabaghlou D, Imani M, Mousazadeh H, Dadashpour M, Firouzi-Amandi A, Zarghami N (2022) Design and fabrication of a dual-drug loaded nano-platform for synergistic anticancer and cytotoxicity effects on the expression of leptin in lung cancer treatment. J Drug Deliv Sci Technol 73:103389

Belo J, Krishnamurthy M, Oakie A, Wang R (2013) The role of SOX9 transcription factor in pancreatic and duodenal development. Stem Cells Dev 22(22):2935–2943. https://doi.org/10.1089/scd.2013.0106

Bezerra DP, Pessoa C, de Moraes MO, Saker-Neto N, Silveira ER, Costa-Lotufo LV (2013) Overview of the therapeutic potential of piplartine (piperlongumine). Eur J Pharm Sci 48(3):453–463. https://doi.org/10.1016/j.ejps.2012.12.003

Carlos JAEG, Lima K, Coelho-Silva JL, de Melo Alves-Paiva R, Moreno NC, Vicari HP, de Souza Santos FP, Hamerschlak N, Costa-Lotufo LV, Traina F (2020) Reversine exerts cytotoxic effects through multiple cell death mechanisms in acute lymphoblastic leukemia. Cell Oncol 43(6):1191–1201. https://doi.org/10.1007/s13402-020-00551-3

Chen Y, Liu JM, Xiong XX, Qiu XY, Pan F, Liu D, Lan SJ, Jin S, Yu SB, Chen XQ (2015) Piperlongumine selectively kills hepatocellular carcinoma cells and preferentially inhibits their invasion via ROS-ER-MAPKs-CHOP. Oncotarget 6(8):6406. https://doi.org/10.18632/oncotarget.3444

Chen YJ, Kuo CC, Ting LL, Lu LS, Lu YC, Cheng AJ, Lin YT, Chen CH, Tsai JT, Chiou JF (2018) Piperlongumine inhibits cancer stem cell properties and regulates multiple malignant phenotypes in oral cancer. Oncol Lett 15(2):1789–1798. https://doi.org/10.3892/ol.2017.7486

Chen SY, Huang HY, Lin HP, Fang CY (2019) Piperlongumine induces autophagy in biliary cancer cells via reactive oxygen species-activated Erk signaling pathway. Int J Mol Med 44(5):1687–1696. https://doi.org/10.3892/ijmm.2019.4324

Collins A, Møller P, Gajski G, Vodenková S, Abdulwahed A, Anderson D, Bankoglu EE, Bonassi S, Boutet-Robinet E, Brunborg G (2023) Measuring DNA modifications with the comet assay: a compendium of protocols. Nat Protoc 18(3):929–989

Domenici G, Aurrekoetxea-Rodríguez I, Simões BM, Rábano M, Lee SY, San Millán J, Comaills V, Oliemuller E, López-Ruiz JA, Zabalza I (2019) A Sox2–Sox9 signalling axis maintains human breast luminal progenitor and breast cancer stem cells. Oncogene 38(17):3151–3169. https://doi.org/10.1038/s41388-018-0656-7

Dudás J, Ladányi A, Ingruber J, Steinbichler TB, Riechelmann H (2020) Epithelial to mesenchymal transition: a mechanism that fuels cancer radio/chemoresistance. Cells 9(2):428. https://doi.org/10.3390/cells9020428

Han SJ, Kwon S, Kim KS (2021) Challenges of applying multicellular tumor spheroids in preclinical phase. Cancer Cell Int 21:1–19

Haynes J, Srivastava J, Madson N, Wittmann T, Barber DL (2011) Dynamic actin remodeling during epithelial–mesenchymal transition depends on increased moesin expression. Mol Biol Cell 22(24):4750–4764. https://doi.org/10.1091/mbc.E11-02-0119

Javan ES, Lotfi F, Jafari-Gharabaghlou D, Mousazadeh H, Dadashpour M, Zarghami N (2022) Development of a magnetic nanostructure for co-delivery of metformin and silibinin on growth of lung cancer cells: possible action through leptin gene and its receptor regulation. Asian Pac J Cancer Prev: APJCP 23(2):519

Kim BN, Ahn DH, Kang N, Yeo CD, Kim YK, Lee KY, Kim T-J, Lee SH, Park MS, Yim HW (2020) TGF-β induced EMT and stemness characteristics are associated with epigenetic regulation in lung cancer. Sci Rep 10(1):10597

Lamouille S, Xu J, Derynck R (2014) Molecular mechanisms of epithelial–mesenchymal transition. Nat Rev Mol Cell Biol 15(3):178–196. https://doi.org/10.1038/nrm3758

Li S, Yang K, Chen X, Zhu X, Zhou H, Li P, Chen Y, Jiang Y, Li T, Qin X (2021) Simultaneous 2D and 3D cell culture array for multicellular geometry, drug discovery and tumor microenvironment reconstruction. Biofabrication 13(4):045013. https://doi.org/10.1088/1758-5090/ac1ea8

Liu D, Qiu XY, Wu X, Hu DX, Li CY, Yu SB, Pan F, Chen XQ (2017) Piperlongumine suppresses bladder cancer invasion via inhibiting epithelial mesenchymal transition and F-actin reorganization. Biochem Biophys Res Commun 494(1–2):165–172. https://doi.org/10.1016/j.bbrc.2017.10.061

Mittal V (2016) Epithelial mesenchymal transition in aggressive lung cancers. Adv Exp Med Biol 890:37–56. https://doi.org/10.1007/978-3-319-24932-2_3

Nayak N, Basha SA, Tripathi SK, Biswal BK, Mishra M, Sarkar D (2021) Non-cytotoxic and non-genotoxic wear debris of strontium oxide doped (Zirconia Toughened Alumina)(SrO-ZTA) implant for hip prosthesis. Mater Chem Phys 274:125187

Nejati K, Rastegar M, Fathi F, Dadashpour M, Arabzadeh A (2022) Nanoparticle-based drug delivery systems to overcome gastric cancer drug resistance. J Drug Deliv Sci Technol 70:103231

Otsuki Y, Saya H, Arima Y (2018) Prospects for new lung cancer treatments that target EMT signaling. Dev Dyn 247(3):462–472. https://doi.org/10.1002/dvdy.24596

Panda M, Tripathi SK, Biswal BK (2021) SOX9: an emerging driving factor from cancer progression to drug resistance. Biochim Biophys Acta Rev Cancer 1875(2):188517. https://doi.org/10.1016/j.bbcan.2021.188517

Pandey K, Tripathi SK, Panda M, Biswal BK (2020) Prooxidative activity of plumbagin induces apoptosis in human pancreatic ductal adenocarcinoma cells via intrinsic apoptotic pathway. Toxicol in Vitro 65:104788. https://doi.org/10.1016/j.tiv.2020.104788

Phi LTH, Sari IN, Yang Y-G, Lee S-H, Jun N, Kim KS, Lee YK, Kwon HY (2018) Cancer stem cells (CSCs) in drug resistance and their therapeutic implications in cancer treatment. Stem Cells Int 2018:5416923. https://doi.org/10.1155/2018/5416923

Pouremamali F, Pouremamali A, Dadashpour M, Soozangar N, Jeddi F (2022) An update of Nrf2 activators and inhibitors in cancer prevention/promotion. Cell Commun Signal 20(1):100

Rajabi S, Maresca M, Yumashev AV, Choopani R, Hajimehdipoor H (2021) The most competent plant-derived natural products for targeting apoptosis in cancer therapy. Biomolecules 11(4):534. https://doi.org/10.3390/Biom11040534

Ranjan A, Ramachandran S, Gupta N, Kaushik I, Wright S, Srivastava S, Das H, Srivastava S, Prasad S, Srivastava SK (2019) Role of phytochemicals in cancer prevention. Int J Mol Sci 20(20):4981. https://doi.org/10.3390/ijms20204981

Shrivastava S, Kulkarni P, Thummuri D, Jeengar MK, Naidu V, Alvala M, Redddy GB, Ramakrishna S (2014) Piperlongumine, an alkaloid causes inhibition of PI3 K/Akt/mTOR signaling axis to induce caspase-dependent apoptosis in human triple-negative breast cancer cells. Apoptosis 19(7):1148–1164. https://doi.org/10.1007/s10495-014-0991-2

Song B, Zhan H, Bian Q, Gu J (2016) Piperlongumine inhibits gastric cancer cells via suppression of the JAK1, 2/STAT3 signaling pathway. Mol Med Rep 13(5):4475–4480. https://doi.org/10.3892/mmr.2016.5091

Sung H, Ferlay J, Siegel RL, Laversanne M, Soerjomataram I, Jemal A, Bray F (2021). Global cancer statistics 2020: GLOBOCAN estimates of incidence and mortality worldwide for 36 cancers in 185 countries. CA: a cancer Journal for Clinicians 71(3):209–249. https://doi.org/10.3322/caac.21660

Tripathi SK, Biswal BK (2018) Pterospermum acerifolium (L.) wild bark extract induces anticarcinogenic effect in human cancer cells through mitochondrial-mediated ROS generation. Mol Biol Rep 45:2283–2294

Tripathi SK, Biswal BK (2020) Piperlongumine, a potent anticancer phytotherapeutic: Perspectives on contemporary status and future possibilities as an anticancer agent. Pharmacol Res 156:104772. https://doi.org/10.1016/J.Phrs.2020.104772

Tripathi SK, Biswal BK (2021) SOX9 promotes epidermal growth factor receptor-tyrosine kinase inhibitor resistance via targeting β-catenin and epithelial to mesenchymal transition in lung cancer. Life Sci 277:119608

Tripathi SK, Panda M, Biswal BK (2019) Emerging role of plumbagin: cytotoxic potential and pharmaceutical relevance towards cancer therapy. Food Chem Toxicol 125:566–582. https://doi.org/10.1016/j.fct.2019.01.018

Tripathi SK, Rengasamy KR, Biswal BK (2020) Plumbagin engenders apoptosis in lung cancer cells via caspase-9 activation and targeting mitochondrial-mediated ROS induction. Arch Pharmacal Res 43(2):242–256. https://doi.org/10.1007/s12272-020-01221-6

Tripathi SK, Sahoo RK, Biswal BK (2022) SOX9 as an emerging target for anticancer drugs and a prognostic biomarker for cancer drug resistance. Drug Discovery Today 27(9):2541–2550. https://doi.org/10.1016/j.drudis.2022.05.022

Yasamineh S, Gholizadeh O, Kalajahi HG, Yasamineh P, Firouzi-Amandi A, Dadashpour M (2023) Future prospects of natural polymer-based drug delivery systems in combating lung diseases. In: Dureja H, Adams J, Löbenberg R, Andreoli Pinto TdJ, Dua K (eds) Natural polymeric materials based drug delivery systems in lung diseases. Springer, Singapore. https://doi.org/10.1007/978-981-19-7656-8_25

Ye X, Weinberg RA (2015) Epithelial–mesenchymal plasticity: a central regulator of cancer progression. Trends Cell Biol 25(11):675–686. https://doi.org/10.1016/j.tcb.2015.07.012

Publisher's Note Springer Nature remains neutral with regard to jurisdictional claims in published maps and institutional affiliations.

Springer Nature or its licensor (e.g. a society or other partner) holds exclusive rights to this article under a publishing agreement with the author(s) or other rightsholder(s); author self-archiving of the accepted manuscript version of this article is solely governed by the terms of such publishing agreement and applicable law.